

## Determination of Plasma Density and Temperature from Intensity Ratios of He I Emission Lines in Diversified Plasma Simulator (DiPS)

Y. H. Jung<sup>1</sup>, J.-S. Yoon<sup>\*1</sup>, S. J. Yoo<sup>1</sup>, Y.-W. Kim<sup>1</sup>, T. Lho<sup>1</sup>, B. Lee<sup>1</sup>, J.-J. Do<sup>2</sup>, H.-J. Woo<sup>2</sup>, and K.-S. Chung<sup>2</sup>

<sup>1</sup> National Fusion R&D Center, Korea Basic Science Institute, Daejeon 305-303, Korea

<sup>2</sup> Electric Probe Applications Laboratory (ePAL), Hanyang University, Seoul 133-791, Korea

Received 23 May 2005, accepted 26 August 2005

Published online 9 June 2006

**Key words** Collisional radiative model, line ratio, neutral helium, plasma edge.

**PACS** 39.30.+w, 52.70.-m, 52.70.Kz

The intensity ratios of He I emission lines are used to determine electron density and temperature in Diversified Plasma Simulator (DiPS). The He I line ratios are measured by optical emission spectroscopy and are calculated using the collisional-radiative equilibrium (CRE) model. The measured He I line ratios are 706.52 nm / 728.13 nm for electron temperature and 728.13 nm / 667.82 nm for electron density determination, respectively. The results obtained from the collisional-radiative equilibrium model are crosschecked with those of electrical probe measurement.

© 2006 WILEY-VCH Verlag GmbH & Co. KGaA, Weinheim

### 1 Introduction

Spectroscopy of radiation emitted from a plasma is a powerful technique for studying the nature of the plasma [1,2] since the signals obtained by spectroscopy contain much information about temperature, density and flux of the main species and impurities. A spectroscopic technique based on the relative intensities of helium lines is used to measure the electron temperature ( $T_e$ ) and density ( $n_e$ ) in the fusion edge plasma [3–6]. This nonintrusive diagnostic relies on the fact that the electron impact excitation rate coefficients for helium singlet and triplet states differ as a function of the electron temperature. In contrast, singlet states differ as a function of the electron density.

Cunningham [7] first applied this line intensity ratio method to measuring electron temperatures in many plasma conditions. Many subsequent workers used measurements that depend on the same principle, but which are refinements of Cunningham's method [8]. Recently, this technique has been considerably improved and extended to high-density, fusion edge plasmas [4,9–11].

At low densities ( $n_e < 10^{11} \text{ cm}^{-3}$ ), the steady-state corona model can be used to determine the electron temperature and density with reasonable accuracy. However, at higher densities ( $n_e > 10^{11} \text{ cm}^{-3}$ ), secondary processes, such as excitation transfer, excitation from metastable are no longer negligible and the steady-state corona model can no longer be used. Under these high-density conditions, collisional-radiative equilibrium models must be used to predict the temperature and density. These complex models take into account many of the secondary processes and no longer assume that excitation is exclusively from the ground state.

Thus, in the present work,  $T_e$  and  $n_e$  measurements using He I emission line intensity ratios based on the collisional-radiative model are applied to the Diversified Plasma Simulator (DiPS) which is for the divertor edge studies. The new versatile linear machine, the DiPS has been developed for divertor edge simulation, space

\* Corresponding author: e-mail: jsyoon@kbsi.re.kr, Phone: +82 42 870 1653, Fax: +82 42 870 1699

propulsion and electric probe technology and its applications. These measurements have been carried out simultaneously with an electric probe system, which gives continuous information on the electron temperature and density.

In this paper, the results of the measurements of  $T_e$  and  $n_e$  by the line-intensity ratio method based on the collisional-radiative equilibrium model are discussed. In section 2 we describe the principle of the line-intensity ratio method and collisional-radiative model. Section 3 contains descriptions of the experimental apparatus. Finally, results and discussions are given in section 3.

## 2 Principle of line-intensity ratio method

In general, the intensity of a spectral line is a function of both electron temperature and density. However, it is possible to identify certain spectral lines which are sensitive to electron temperature (density) but not electron density (temperature). Such spectral lines can be very useful diagnostics of plasma electron temperature and density. However, the link between measured line intensity ratio and plasma electron temperature and density is complex and a number of issues must be examined for the diagnostics. In particular, the different processes associated with the formation of excited level populations responsible for the chosen atomic transitions must be understood well in order to extract information relative to the electron temperature and density of the plasma.

The plasma emissivity  $\epsilon_{qp}$  (power emitted per unit time per unit volume per unit solid angle) at a specific wavelength  $\lambda_{qp}$  corresponding to an atomic transition from level  $q$  to level  $p$  can be written as [12]

$$\epsilon_{qp} = \frac{h\nu_{qp}}{4\pi} n_q A_{qp}, \quad (1)$$

where  $h\nu_{qp}$  is the photon energy associated to the transition,  $n_q$  is the population of the emitting level,  $A_{qp}$  is the Einstein coefficient for the transition. Assuming a uniform plasma and no reabsorption of photons within the plasma, measured intensity  $I_{qp}(\lambda_{qp})$  at specific wavelength  $\lambda_{qp}$  is given by

$$I_{qp}(\lambda_{qp}) = \frac{1}{4\pi} n_q A_{qp} V \Omega T(\lambda_{qp}) \eta(\lambda_{qp}), \quad (2)$$

where  $V$  is the plasma volume,  $\Omega$  is the solid angle subtended by the collection optics,  $T(\lambda_{qp})$  and  $\eta(\lambda_{qp})$  are the transmission factor of the detector system and the quantum efficiency at wavelength  $\lambda_{qp}$ , respectively. Thus intensity ratios for two lines is

$$\frac{I_{qp}(\lambda_{qp})}{I_{ji}(\lambda_{ji})} = \frac{n_q A_{qp} T(\lambda_{qp}) \eta(\lambda_{qp})}{n_j A_{ji} T(\lambda_{ji}) \eta(\lambda_{ji})} = \frac{1}{C} \frac{n_q A_{qp}}{n_j A_{ji}}, \quad (3)$$

where  $C$  is the relative calibration factor (ratio of the responses of the detection system at the two wavelengths).

At low densities ( $n_e < 10^{11} \text{ cm}^{-3}$ ), the steady-state corona model can be used to predict the population of excited levels provided the plasma condition satisfies the applicability criteria for the model. The steady-state corona model assumes that line emission is the result of single collisions between electron and atoms in the ground state followed by the direct radiative de-excitation. Thus in this model, a balance between the rate of collisional excitation from the ground state and the rate of spontaneous radiative decay determines the population densities of the excited levels. Then, the population of the level  $q$  ( $N_q$ ) is given by the expression [8]:

$$n_e n_0 \langle \sigma v \rangle_{0q} = n_q \sum_{p < q} A_{qp}, \quad (4)$$

where  $n_0$  is the population of the ground level population,  $n_e$  is the electron density,  $\sum_{p < q} A_{qp}$  is the total transition probability from level  $q$  to all lower states, and  $\langle \sigma v \rangle_{0q}$  is the excitation rate coefficient for the electron impact excitation of the level  $q$  from ground state. Thus, the line ratio expressed in terms of excitation rate coefficients in the steady-state corona model becomes

$$\frac{I_{qp}(\lambda_{qp})}{I_{ji}(\lambda_{ji})} = \frac{1}{C} \frac{E_{qp}(T_e)}{E_{ji}(T_e)}, \quad (5)$$

where  $E_{qp}(T_e)$  is the emission rate coefficient. In this model, the line intensity ratio depends only on the electron temperature in the plasma. The steady-state corona model is believed to be able to predict the electron temperature

with reasonable accuracy for electron densities up to  $10^{11}\text{cm}^{-3}$ . However, at higher densities, this assumption is no longer valid since the occurrence of secondary processes involving collisions with excited or ionized atoms become important. These contributions can be integrated in the line ratio expression by replacing the emission rate coefficients by an apparent or resulting emission rate coefficient  $E_{qp}^*(T_e, n_e)$  and  $E_{ji}^*(T_e, n_e)$  that include both direct (ground) and indirect (metastables) excitation:

$$\frac{I_{qp}(\lambda_{qp})}{I_{ji}(\lambda_{ji})} = \frac{1}{C} \frac{E_{qp}^*(T_e, n_e)}{E_{ji}^*(T_e, n_e)}. \quad (6)$$

Collisional radiative models are 0-dimensional plasma models, used to calculate atomic state distribution functions for one or more species, as a function of particle temperatures and densities. They normally work under the assumption that the two main types of processes that cause an atom to charge its excited state are radiative processes and electron collisions. These models can be an useful tool in understanding experimental observations, for instance to relate an observed spectrum to an atomic state distribution function, and thus to an electron density and temperature. In addition, a collisional radiative model can be used to calculate effective ionization and recombination rates, and the effective emissivity, as a function of electron temperature and density.

In order to use collisional radiative models normally one assumes that the free electrons have a Maxwellian velocity distribution, and the plasma is optically thin, especially to its own resonance radiation. In addition, the ionization process is by electron collision from any bound level and is partially balanced by three-body recombination into any level, excitation transfer between any pair of bound levels are induced by electron collisions and radiation is emitted when a bound electron makes a spontaneous transition to a lower level or when a free electron makes a collisionless transition into a bound level. With these assumptions, we now consider ionization and recombination of a plasma and the population densities of various atomic levels in it under a given plasma condition, which is specified by electron and ion densities,  $n_e$  and  $n_i$ , respectively, and by the electron temperature,  $T_e$ . The time development of the population density of a level  $p$  is described by the differential equation

$$\begin{aligned} \frac{dn_p}{dt} = & - \left\{ \sum_{q \neq p} C_{pq} n_e + \sum_{q < p} A_{pq} + S_p n_e \right\} n_p \\ & + \sum_{q \neq p} \{ C_{qp} n_e + A_{qp} \} n_q + \{ \alpha_p n_e + \beta_p \} n_i n_e, \end{aligned} \quad (7)$$

where  $C_{pq}$  is the rate coefficient for excitation ( $p > q$ ) or de-excitation ( $q < p$ ) by electron collisions from a level  $p$  to  $q$ ,  $A_{pq}$  is the spontaneous transition probability from  $p$  to  $q$ ,  $S_p$  and  $\alpha_p$  are the rate coefficients for ionization by electron collisions from  $p$  and its inverse three-body recombination coefficient to this level, respectively, and  $\beta_p$  is the radiative and dielectronic recombination coefficient to this level. The summation  $q > p$  means the sum over levels  $q$  having higher energy than  $p$ . Other processes such as induced emission are neglected. In this paper, we use a collisional radiative model to evaluate the excited state populations of helium.

### 3 Experiment

A new versatile linear machine, called DiPS (Diversified Plasma Simulator) has been developed for the divertor edge simulation, space propulsion and electric probe technology and its applications. The schematic drawing of the DiPS device is shown in Fig. 1. To verify and develop theories of electric probes with magnetic field, collisionality, various particle sources, and wide range of plasma parameters, one needs a plasma source with the following plasma parameters: density =  $10^6 \sim 10^{14}\text{cm}^{-3}$ , electron temperature =  $1 \sim 10$  eV, magnetic field =  $0 \sim 2$  kG, plasma types = RF and DC. For these conditions, the DiPS is developed with two plasma sources, LaB<sub>6</sub>(DC) and Helicon plasma (RF). The LaB<sub>6</sub> cathode used in DiPS consists of disk-type LaB<sub>6</sub> which is heated indirectly by the graphite heater up to 5 kW. The discharge voltage and current are  $1 \sim 100$  V and  $1 \sim 50$  A, respectively. The helicon plasma source also is developed as a high density rf plasma source in DiPS, which generates the high density plasma with the of power of 0-3kW by using an  $m = 0$  antenna.

The experimental apparatus is composed of a discharge chamber (test chamber region shown in Fig. 1), a spectroscopy system, a fast scanning probe system with a single probe. The fast scanning probe system, which

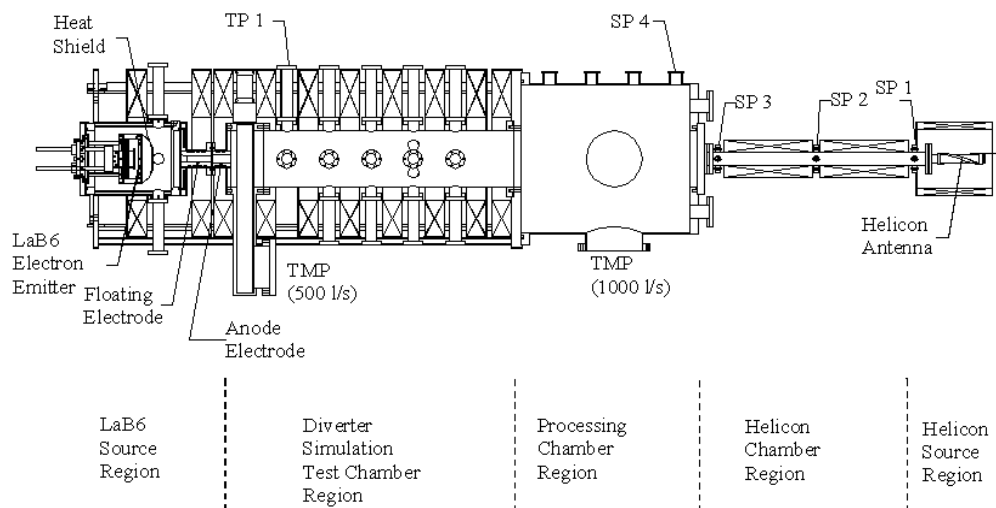


**Fig. 1** Schematic drawing of the DiPS device

is driven by a pneumatic cylinder with stroke of  $5 \sim 10$  cm, measures the electron temperature and the plasma density by using a single probe (0.025 mm in diameter, 1.4 mm in length). The spectroscopy system is composed of a monochromator, an optical multichannel analyzer (OMA), and an optical fiber. The monochromator has a 500 mm focal length and a 0.05 nm resolution. The spectral response of the OMA is  $300 \sim 900$  nm at  $1024 \times 128$  pixels.

Experiments were performed at test chamber pressure of  $2.0 \times 10^{-3}$  torr, magnetic field of 400 G. The plasmas were measured using the fast scanning probe system and the optical emission spectroscopy system. The fast scanning probe system with a single probe had an average operating speed of  $0.4 \sim 0.7$  m/sec and a maximum speed of 2.2 m/sec, was used to measure the plasma electron temperature and density. The optical emission spectroscopy system with a monochromator received the light emitted from the plasma. The line radiation of the excited He-atoms is measured at three different wavelengths. We selected two transitions in the singlet system ( $3d^1D \rightarrow 2p^1P$ ) at 667.82 nm and ( $3s^1S \rightarrow 2p^1P$ ) at 728.13 nm and one in the triplet system ( $3s^3S \rightarrow 2p^3P$ ) at 706.52 nm. The ratio of the line intensities in the singlet system (728.13 nm / 667.82 nm) is most sensitive to the electron density whereas the ratio of the line intensities in the triplet and singlet system (728.13 nm / 706.52 nm) is strongly depend on the electron temperature. More detailed line selection procedures are discussed in next section.

## 4 Results and discussions

In order to measure the electron temperature and density from a line ratio, a careful selection of electron of emission lines must be made. First, the line ratio of the selected transitions must be insensitive to density variation to be applied for the determination of temperature. In contrast, selected transitions must be insensitive to temperature variation to be used for the determination of density. Also, secondary effects depend on the density, thus we must select transitions for which secondary effects have limited importance on the resulting intensities for temperature determination.

The He Grotrian diagram is shown in Fig. 2. The left side of the diagram features the singlet states while the triplet states are shown in the right side. The He atom has 2 metastables, namely the  $2^1S$  state (singlet) and the  $2^3S$  state (triplet). The energy levels of the He atom are given in Table 1. As seen in the Grotrian diagram, there are a number of possible transitions that can be used. Transitions originating from a level with principal quantum number  $n > 5$  will not be considered since the electron population of these higher levels becomes increasingly smaller with increasing  $n$ , resulting in weak transitions. Transitions ending at the ground state  $1^1S$

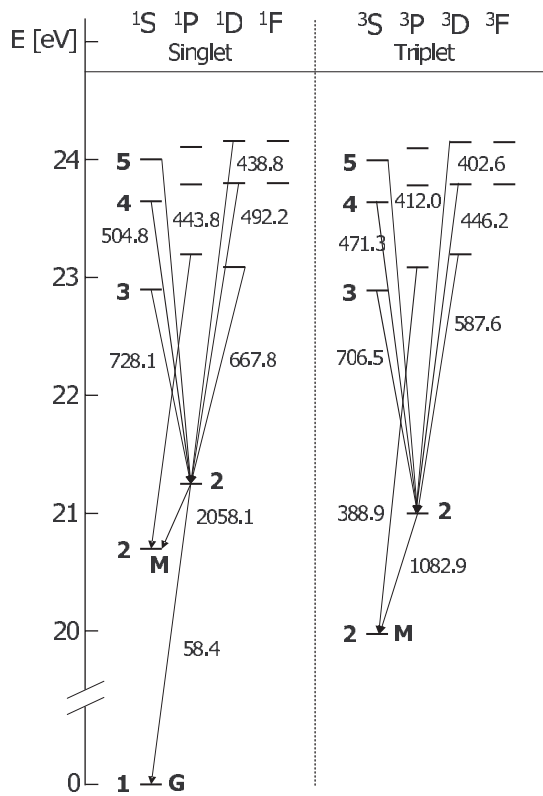


**Table 1** Helium energy levels. Singlet (left) and triplet (right) states.

Level	Energy (eV)	Level	Energy (eV)
$2^1S$	20.610	$2^3S$	19.814
$2^1P$	21.212	$2^3P$	20.958
$3^1S$	22.914	$3^3S$	22.712
$3^1P$	23.081	$3^3P$	23.001
$3^1D$	23.068	$3^3D$	23.067
$4^1S$	23.667	$4^3S$	23.588
$4^1P$	23.736	$4^3P$	23.730
$4^1D$	23.730	$4^3D$	23.730
$4^1F$	23.731	$4^3F$	23.731
$5^1S$	24.005	$5^3S$	23.965
$5^1P$	24.039	$5^3P$	24.022
$5^1D$	24.036	$5^3D$	24.036
$5^1F$	24.037	$5^3F$	24.037

**Fig. 2** Partial Grotrian diagram of the helium atom with some important transitions ( $\lambda$  in nm). G and M are for ground and metastables states, respectively.

and at metastable level  $2^1S$  and  $2^3S$  will not be considered since the plasma is not optically thin with respect to these transitions and the resulting intensities are strongly affected by re-absorption.

In order to measure the electron density,  $D \rightarrow P$  transitions are better suited in two reasons. First, excitation transfer cross sections for allowed transitions are much larger than for non-allowed transitions. Second, the excitation transfer is inversely proportional to the energy difference between levels and strongly dependent on plasma density. For example, the energy difference between the  $3^1P$  and  $3^1D$  level is only 0.013 eV while the corresponding quantity between the  $3^3P$  and  $3^3D$  levels 0.066 eV. For the  $n = 4$  level,  $\Delta E(4^1P/4^1D)$  is only 0.006 eV while  $\Delta E(4^3P/4^3D)$  is even smaller. Thus these transitions will be more sensitive to plasma density than electron temperature. For these reasons, we measured HeI line ratios of 728.13 nm ( $3s^1S \rightarrow 2p^1P$ ) / 667.82 nm ( $3d^1D \rightarrow 2p^1P$ ) for electron density determination.

Line ratios using  $S \rightarrow P$  transitions are better suited to measure electron temperature. The contributions from the metastable  $2^1S$  and  $2^3S$  states due to excitation transfer are small since these  $s \rightarrow$  transitions are forbidden and the resulting cross sections are small. Also, for a given  $n$  level, the energy of the  $S$  levels is significantly different than the energy of the other  $P$ ,  $D$ , or  $F$  levels. Thus excitation transfer cross sections between  $S$  and any of these  $P$ ,  $D$ , or  $F$  levels are also small compared to cross section involving only  $P$ ,  $D$ , and  $F$  levels. For these reasons, 728.13 nm ( $3s^1S \rightarrow 2p^1P$ ) / 706.52 nm ( $3s^3S \rightarrow 2p^3P$ ) ratio is attractive for electron temperature determination.

The two transitions in the singlet system ( $3d^1D \rightarrow 2p^1P$ ) at 667.82 nm and ( $3s^1S \rightarrow 2p^1P$ ) at 728.13 nm and one in the triplet system ( $3s^3S \rightarrow 2p^3P$ ) at 706.52 nm have been selected. The ratios of the line intensities are compared with those calculated in a collisional-radiative equilibrium model for given plasma parameters. In

order to predict the electron temperature and density, here we consider a two-dimensional test function as

$$f(T_e, n_e) = \sum_i \left( \frac{R_i^{\text{exp}} - R_i^{\text{cal}}(T_e, n_e)}{R_i^{\text{exp}}} \right)^2, \quad (8)$$

where the summation is over the pairs 728.13 nm / 667.82 nm and 728.13 nm / 706.52 nm.  $R_i$  is the line intensity ratio and the superscripts “exp” and “cal” indicate the experimental and calculational values, respectively. The electron temperature ( $T_e$ ) and density ( $n_e$ ) are simultaneously obtained so as to minimize the test function, Eq. 8. Fig. 3 shows the results. It is found that the electron temperature and density profiles which are calculated by line ratio method based on the collisional-radiative equilibrium model have good agreement with the values which are measured by a fast scanning probe.

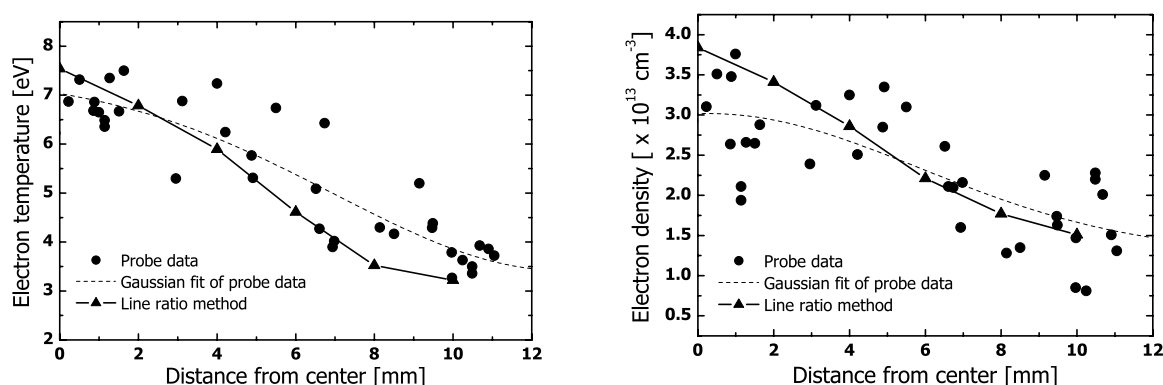


**Fig. 3** Electron temperature and density profiles obtained with the He I line intensity ratio method and with fast scanning probe.

## References

- [1] I.H. Hutchinson, *Principles of Plasma Diagnostics*, second ed. (Cambridge University Press, Cambridge, 2002).
- [2] H.R. Griem, *Plasma Spectroscopy* (McGraw-Hill, New York, 1965), pp. 243 - 253.
- [3] R. Mewe, *Brit. J. Appl. Phys.* **18**, 107 (1967).
- [4] B. Schweer, G. Mank, A. Pospieszczyk, B. Brosda, and B. Pohlmeier, *J. Nucl. Mater.* **196-198**, 174 (1995).
- [5] R.F. Biovin, J.L. Kline, and E.E. Scime, *Phys. Plasmas* **8**, 5303 (2001).
- [6] N.K. Podder et al., *Phys. Plasmas* **11**, 5436 (2004).
- [7] S.P. Cunningham, in *Conf. on Thermonuclear Reactors*, Livermore, U. S. Atomic Energy Commission Rep. **279**, 289 (1955).
- [8] R.W.P. McWhiter, *Plasma Diagnostic Techniques*, ed. R. H. Huddleston and S. L. Leonard (New York, Academic, 1965) ch. 5.
- [9] S.J. Davies, P.D. Morgan et al., *J. Nucl. Mater.* **241-243**, 426 (1997).
- [10] Y. Andrew, S.J. Davies et al., *J. Nucl. Mater.* **266-269**, 1234 (1999).
- [11] Y. Andrew and M.G. O'Mullane, *Plasma Phys. Controlled Fusion*, **42**, 301 (2000).
- [12] W.L. Wiese, M.W. Smith, and B.M. Glennon, *Atomic Transitions Probabilities*, vol. 1, National Standard Reference Data System NSRDS-NBS-4 (1996).